The Relationship between Peptide Plane Rotation (PPR) and Similar Conformations

J. M. R. PARKER

API Alberta Peptide Institute, Department of Biochemistry, University of Alberta, Edmonton, Alberta, Canada T6G 2S2

Received 30 June 1998; accepted 8 February 1999

ABSTRACT: Currently, several energy functions and conformational search methods have been developed that are based on the observed distribution of phi and psi angles in protein structures. The definition of phi and psi angles is directly related to the orientation of the peptide plane (CA—CO—NH—CA). Starting from one conformation and rotating a single peptide plane, the angles psi for one residue and phi for the consecutive residue that are linked by the peptide plane, display a continuous range of values within one global conformation. When peptide plane rotation is analyzed in several different conformations generated from a restricted conformation database, a large number of these conformations are related. Based on these observations, a new simplified all-atom representation for protein folding simulations is presented where only one torsion angle variable is required for each residue. The underlying theme of this article is that conformational search methods using phi and psi torsion space, search through many redundant conformations. These conformations are related by anticorrelated torsion changes of peptide plane rotations. © 1999 John Wiley & Sons, Inc. J Comput Chem 20: 947–955, 1999

Keywords: peptide plane rotation; conformational search; Levinthal paradox; simplified search algorithm; one torsion angle variable

Correspondence to: J. M. R. Parker; e-mail: bob.parker@ualberta.ca

This article includes Supplementary Material available from the authors upon request or via the Internet at ftp.wiley.com/public/journals/jcc/suppmat/20/947 or http://journals.wiley.com/jcc/

CCC 0192-8651 / 99 / 090947-09

Introduction

Two fundamental assumptions used to study protein folding are the ''thermodynamics hypothesis,'' where the native structure is the lowest Gibbs free energy structure,[1] and the ''Levinthal Paradox,'' where a limited number of conformations are searched in the protein folding pathway.[2–5] In both of these areas, several energy functions and conformational search methods have been developed that rely on the distribution of phi and psi angles observed in protein X-ray structures.

Protein conformations have been predicted using methods such as energy minimization with fixed geometry, Monte Carlo, simulated annealing and molecular dynamics,[6–9] genetic algorithms,[10] and, more recently, fold recognition.[11] Simplified models, such as pseudodihedral[12–15] domain folding[16,17] and lattice models,[18] which reduce the number of atoms and the number of degrees of freedom, are some of the methods that have been used to sample protein conformational space more efficiently.

Torsion angle dynamics, which represents 1/10 of the total degrees of freedom in protein simulations, accounts for most of the large-scale motions in protein.[19] Because of this, many recent studies in the simulation of protein folding have used reduced conformational databases. These databases are derived from the observed distribution of phi and psi angles in proteins and are used to provide a restricted but directed search of protein backbone conformations.[14,20–26] However, it has been reported that protein structure prediction based on reduced dihedral angle databases must be more accurate for protein structure prediction.[27]

This article describes the geometry of peptide plane rotations, where the local motions of different peptide plane orientations are not accompanied by large global conformational changes, as might be expected. Although there is a wide range of phi and psi torsion angles observed in these local motions, all of these conformations are similar because they are related by peptide plane rotations. This suggests that the large number of torsion angles used in conventional conformational search methods can be reduced to a substantially smaller number of torsion angle variables if peptide plane rotation is taken into account. The first part of this article demonstrates that rotation of a single peptide plane in a right-hand alpha-helix does not change the global conformation significantly. The second part shows that multiple phi/psi values in a restricted conformational database are redundant, because many angles describe similar conformations. The third part of this article describes how these observations are used to present a new simplified model of the peptide backbone that can be used to simulate protein folding.

Peptide Plane Rotation in Peptide Conformations

The backbone of a peptide can be described by the positions of the heavy atoms N(i), CA(i), C(i), and O(i) of a residue labeled i, with rigid geometry values for bond distances and bond angles.[28,29] The value of phi is defined by the dihedral angle NH(i)—N(i)—CA(i)—C(i), and the psi angle is defined by N(i)—CA(i)—C(i)—N($i+1$).[30,31] The orientation of the peptide plane can be defined by the plane of the heavy atoms CA(i), C(i), O(i), N($i+1$), and CA($i+1$). This orientation can also be defined by the angle psi of residue i, with rotation about atoms CA(i) and C(i), and the angle phi of residue $i+1$ with rotation about atoms N($i+1$) and CA($i+1$). Rotation about either a single phi (N—CA) or psi (CA—C) bond of a peptide conformation defined by rigid geometry bond angles and bond distances, produces a large global conformational change.[32] Recently, conformational search methods that use two or more angles to allow for local motion without large changes in global conformations have been described.[33]

Because the CA(i)—C(i) and N($i+1$)—CA($i+1$) bonds are nearly parallel, a cooperative change of psi(i) together with phi($i+1$) was investigated in this article as a possible source of local movement without large global movement.[13,34–35] This local movement corresponds to a peptide plane rotation (PPR). It is not immediately apparent that such a local move (peptide plane rotation) will not change the global conformation, because these two bonds are displaced by approximately 1 angstrom from a collinear arrangement. However, in the extreme simplification that these two bonds are collinear, it is straightforward to visualize that any rotation of psi(i) together with an equal but opposite rotation of phi($i+1$) will maintain a global conformation. This simplification is similar to the replacement of the peptide plane by a virtual bond

or pseudodihedral angle[12–15] where the path of consecutive CA atoms can be described by psi(i) + phi($+1$).[12]

For dipeptide structures using rigid geometry bond angles and bond distances, the frame-shifted[34] psi(i) and phi($i + 1$) values have been shown to incorporate conformational information and chain growth direction for two consecutive amino acids.[36] This is unlike the conventional torsion angle description of phi(i) and psi(i), which describe the backbone conformation of only one residue. Figure 1 represents frame-shifted plots of the relationship, psi(i) and phi($i + 1$), for dipeptide conformations starting from phi/psi torsion values of the right-hand helix [$-60/-40$, phi($i + 1$)/psi(i), line labeled A], left-hand helix [60/40, phi($i + 1$)/psi(i), line labeled B], and extended conformation [$-140/140$, phi($i + 1$)/psi(i), line labeled C]. Using the rule psi(i) = $-$phi($i + 1$), points are drawn starting from the torsion angle values listed above. For example, using the right-hand helix as a starting conformation, and incrementing the values of psi and phi by 40 degrees, the values for psi(i) and phi($i + 1$) are $-40/-60$, $0/-100$, $40/-140$, 80/180, 120/140, 160/100, $-160/60$, $-120/20$, and $-80/-20$. These values are plotted to give the line A shown in Figure 1. For a regular repeating structure, these values would correspond to the phi(i) and psi(i) values of $-60/-40$, $-100/0$, $-140/40$, 180/80, 140/120, 100/160, $60/-160$, $20/-120$, and $-20/-80$ in the more traditional dihedral angle description of peptide conformations. These values represent regular repeating helical structures where each residue has the same conformational torsion angle value. The resulting diagonal trends for psi(i) and phi($i + 1$) shown in Figure 1 are similar to the diagonal lines of helical parameter variation of phi and psi values with equivalent number of residues per turn(n),[30] to the diagonal lines that describe the change in peptide torsion angles in the frame-shifted representation of phi and psi,[34] to the diagonal lines that describe the angle between planes of adjacent peptide planes,[35] and to the rotation superposition angle that describes the relationship of adjacent peptide planes.[37] All of these relationships describe contour maps for conformations that are related by different orientations of the peptide plane.

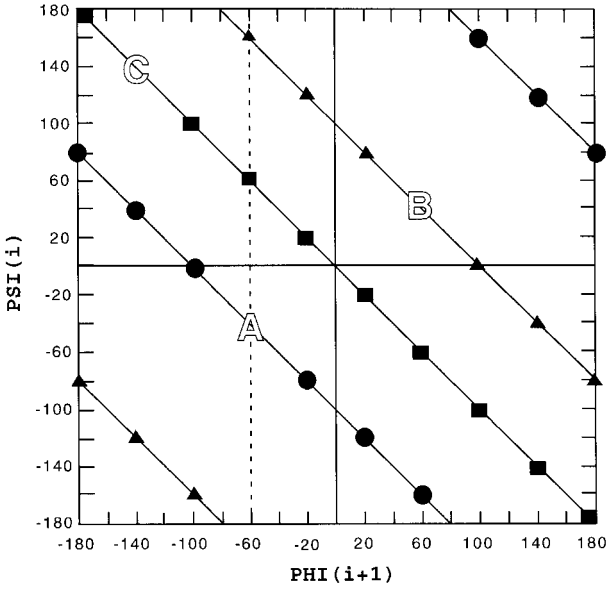

FIGURE 1. Dihedral angle frame-shifted plot of psi(i) (ordinate) and phi($i + 1$) (abscissa). The diagonal line labeled A was drawn from psi = -40 and phi = -60 (circle) and plotted in 40-degree increment changes of psi(i) and phi($i + 1$) for the points $-40/-60$, $0/-100$, $40/-140$, 80/180, 120/140, 160/100, $-160/60$, $-120/20$, and $-80/-20$. The diagonal lines labeled B and C were plotted similarly starting from 40/60 (triangles) and $140/-140$ (squares), respectively. The dotted line at phi = -60, represents the phi value of frame-shifted values for all of the diagonal lines. For example, the frame-shifted values [psi(i), phi($i + 1$)] are $-40/-60$ for line A, $60/-60$ for line C and $160/-60$ for line B.

To graphically show that peptide plane rotations describe similar conformations for one of the frame-shifted contour lines in Figure 1, tetra-peptide conformations were generated using the Biopolymer module in InsightII (Biosym) with the torsion angles described above (Table I) and rigid geometry values for bond distances and bond angles. From the initial conformation of a right-hand alpha-helix, where each residue has phi = -60 and psi = -40 (letter A, Fig. 1), tetra-peptide structures were generated by incrementing torsion values of psi(2) and phi(3) by 40 degrees with the rule that psi(2) = $-$phi(3). The phi and psi values for these dipeptide torsion values [psi(2), phi(3)] listed in Table I, all fall on the line labeled A in Figure 1 in the frame-shifted version of the Ramachandran plot.[34]

Figure 2 shows that the conformations of these tetra-alanine peptides, which were generated from the right-hand alpha-helix by changing only the values of psi(2) and phi(3), are all similar. The heavy atoms of these structures are shown superimposed onto a right-hand helix with phi/psi values of $-60/-40$. It can be seen that all of these

TABLE I.
Peptide Plane Rotation.

Plane Rotation	Residue (2)	Residue (3)	RMSD
0	−60/−40	−60/−40	0.0000
40	−60/0	−100/−40	0.3597
80	−60/40	−140/−40	0.6590
120	−60/80	−180/−40	0.8795
160	−60/120	140/−40	1.0127
200	−60/160	100/−40	1.0439
240	−60/−160	60/−40	0.9519
280	−60/−120	20/−40	0.7220
320	−60/−80	−20/−40	0.3814

The first column lists the rotation (in 40-degree increments) applied to psi(2) and −40-degree increments applied to phi(3) torsion values of the right-hand alpha-helix tetra-alanine peptide, to generate the structures shown in Figure 2. The all-atom RMSD for each structure, compared to the reference right-hand alpha-helix, is shown in column 4.

conformations are similar, except for the orientation of the peptide plane between residues 2 and 3. It should be noted that the RMSD values listed in Table I for these conformations do not reflect their apparent similarity because most of the deviations in atom positions between conformations are due to the atoms of the peptide plane. This large local atom deviation with peptide plane rotation is a direct consequence of the bonds CA(i)—C(i) and N($i + 1$)—CA($i + 1$), because they are nearly parallel but not collinear. In all of these simulations of peptide plane rotation, the N-terminal (N—CA) bond direction and C-terminal (CA—CO) bond direction are similar for all of the intermediate peptide plane rotation conformations. These bond orientations describe the direction of a growing peptide chain or the global conformation. Similar results for single peptide plane rotation in the left-hand alpha-helix, extended conformations and beta turns with anticorrelated movements of both psi(i) and phi($i + 1$) confirmed that there was little change in the global conformation.

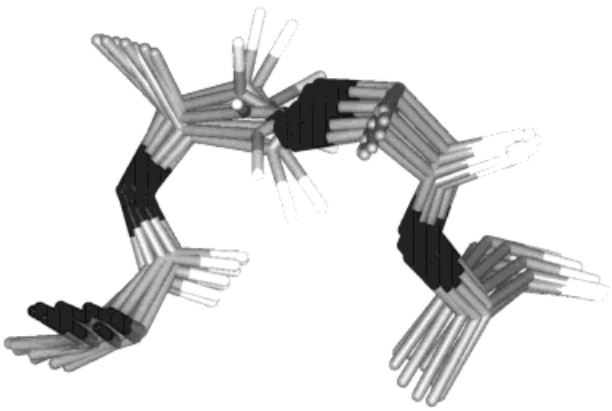

FIGURE 2. Superimposed conformations of nine structures where the value of all psi(i) and phi($i + 1$) have been incremented by 40 degrees, and follow the rule psi(i) = −phi($i + 1$) starting from the right-hand alpha-helix conformation with the torsion angle values of −40/−60 (psi(i)/phi($i + 1$). In this and subsequent figures, the following color scheme is used, nitrogen (black), oxygen (white), and carbon (gray).

There are several reports in the literature that multiple values of phi/psi may represent similar conformations. It has been recognized for some time that type 1 and type 2 beta turns are related by a 180-degree change of the peptide plane orientation. However, this observation has not previously been extended to other conformations. Studies using a one variable beta-turn topological descriptor[38] called beta (C1—CA2—CA3—N4), have shown that there is a significant overlap between all of the beta-turn conformations that is not apparent from the different beta-turn classifications based on phi and psi angles. Also, investigations of the loop-closure problem in peptide conformations[39] have shown that several torsion angle solutions in alpha-helices are observed using either rigid or flexible peptide geometry values. In another report, concerted transitions of psi($i - 1$) and phi(i) were reported, where the peptide plane was rotated by 180 degrees and the backbone and side-chain directions were similar.[40] It is also interesting that T1 measurements and conformational search procedures suggest that local backbone dihedral angles accompany rapid hydrogen bond exchange.[41]

Multiple Values of Phi/Psi Describe Similar Conformations

For the single example of peptide plane rotation in a right-hand helix shown above, the values of psi($i + 1$) and phi($i + 2$) (Table I, residues 2 and 3) would imply that very different conformations are involved. However, taking peptide plane rotation into account, all of these conformations describe similar global conformations when superimposed onto one another (Fig. 2). The implications of peptide plane rotation are elaborated with dipeptide conformations to show that protein conformational search methods that use the full phi/psi conforma-

tional search space or those that use a restricted conformational database, may describe many similar global conformations that are related by the peptide plane rotation. The small, restricted data set reported by Rooman and coworkers[21] will be used as an example. The Rooman database describes six conformations (excluding proline, −117/142, −69/140, −89/− 1, −65/− 40, 78/20, and 103/− 176) for all residues. These 6 psi(i) and 6 phi($i + 1$) angles were combined to generate the 36 dipeptide conformations that are listed in Table II. The 36 structures, generated with these phi and psi values, were superimposed using the heavy atoms, N(i), CA(i), CB(i), C(i), O(i), N($i + 1$), CA($i + 1$), CB($i + 1$), C($i + 1$), O($i + 1$). Visual inspection of all structures and RMSD values, compared to the right-hand alpha-helix value (Table II, column 5) revealed that many of these 36 conformations were similar and could be grouped into four conformational groups (Table II, groups 1 to 4). The RMSD values, listed in column 4 of Table II, show the similarity of each member of a group to one member of that group. A more significant observation was that conformations in groups 1 and 3 were related by rotation about the CA(i) and CA($i + 1$) axis. Similarly, groups 2 and 4 were related by rotation about the CA(i) and CA($i + 1$) axis. To display the similarity of the subgroups within the two main groups, the dipeptide structures shown in Figure 3 were superimposed using the peptide plane atoms. The top figure represents the superimposed conformations for groups 1 and 3, and the bottom figure represents the superimposed conformations for groups 2 and 4. The most important result of this grouping is that all of the conformations within each of these two major groups were found to have similar end terminal bond directions (N(i)—CA(i) and CA($i + 1$)—CO($i + 1$)). These bond directions define the direction of peptide chain growth or the global conformation. In addition, it is important to note that the CA—CB bond directions (side chains) and N-terminal bond directions for groups 1 and 3 (top figure) differed by 180 degrees to that for groups 2 and 4 (bottom figure). This means that there are two major groups of conformations in this conformation database. Within each major group there are some variations in the positions of the N-terminal nitrogen atoms and C-terminal carbonyl atoms. Figure 3 shows that there are two subgroups of N-terminal bond directions within each of the two major groups. In the top figure the N-terminal bond directions furthest to the left are from group 1, while the inner group of N-terminal bond directions, pointing out of the plane of the paper, are from group 3. These two directions are the result of the bond angles N—CA—C associated with the different peptide plane orientations for group 1 compared to group 3. The angle between these two N-terminal bond direction groups ranges from 30 to 40 degrees. This range of values is similar for

TABLE II.

Group	psi(i)	phi($i + 1$)	RMSD	RMSD
	140	−117	0.1839	1.1868
	142	−117	0.0000	1.1939
	−176	−117	0.3817	1.2470
	140	−69	0.4866	1.1625
	142	−69	0.4967	1.1626
1	−176	−69	0.7559	1.0576
	140	−89	0.2782	1.1707
	142	−89	0.2909	1.1744
	−176	−89	0.5826	1.1358
	140	−65	0.5287	1.1613
	142	−65	0.5388	1.1605
	−176	−65	0.7898	1.0436
	−40	−117	0.3539	0.5472
	−1	−117	0.0000	0.4500
	20	−117	0.1924	0.5014
	−40	−69	0.4199	0.0420
	−1	−69	0.5012	0.3244
2	20	−69	0.6232	0.5055
	−40	−89	0.3038	0.2582
	−1	−89	0.2890	0.2940
	20	−89	0.4250	0.4437
	−40	−65	0.4500	0.0000
	−1	−65	0.5437	0.3475
	20	−65	0.6621	0.5264
	−40	78	0.3409	1.5240
	−1	78	0.0000	1.7122
3	20	78	0.1873	1.6033
	−40	103	0.2972	1.7601
	−1	103	0.2768	1.5566
	20	103	0.4078	1.4655
	140	78	0.1872	1.1494
	142	78	0.0000	1.1459
4	−176	78	0.3672	1.1268
	140	103	0.2644	1.1743
	142	103	0.2723	1.1753
	−176	103	0.5550	1.2464

All 36 dipeptide conformations using six conformations per residue as described by Rooman listed as four conformational groups 1, 2, 3, and 4 (column 1). The psi(i) and phi($i + 1$) torsion values are listed in columns 2 and 3. The all-atom RMSD of all structures listed in column 4, are listed relative to one member of each group. The all-atom RMSD of all structures listed in column 5 are listed relative to the reference righ-hand alpha-helix conformation [−40/− 65 psi(i), phi($i + 1$)].

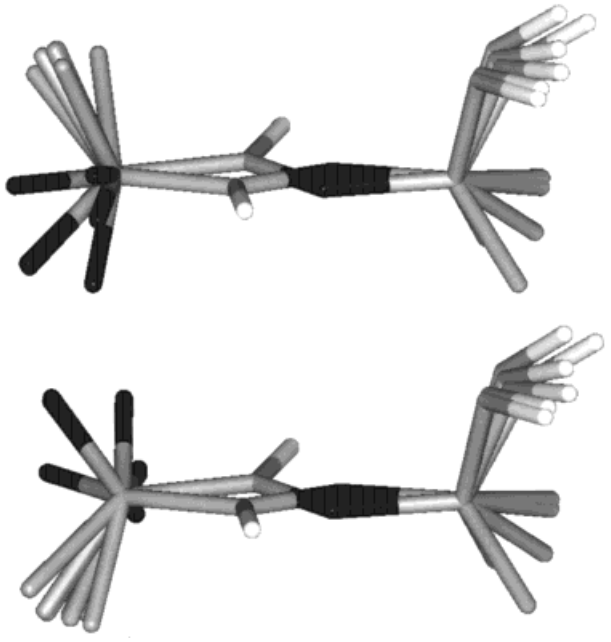

FIGURE 3. All dipeptide structures generated with a restricted conformation dataset of six conformations per residue, superimposed into two groups. The top figure represents 18 superimposed structures from groups 1 and 3 (Table II). The bottom figure represents 18 superimposed structures from groups 2 and 4 (Table II). The N-terminal atoms are to the left, while the C-terminal atoms are to the right. The CA and C-terminal CO atoms are in the plane of the paper; the peptide plane carbonyl/nitrogen and N-terminal nitrogen atoms point into and out of the plane of the paper. In the top figure, the peptide plane carbonyls of group 1 and group 3 point out of and into the plane of the paper, respectively. In the bottom figure, the peptide plane carbonyls of group 2 and group 4 point out of and into the plane of the paper, respectively.

the N-terminal bond directions in the bottom figure. It is interesting to note that the peptide backbone covalent geometry is conformation dependent,[42] with bond angle variation of several degrees from standard values.

To summarize these results, all 36 Rooman dipeptide conformations can be grouped into two similar conformations, one characterized by right-hand alpha-helix torsion values (groups 2 and 4) and the other by extended torsion angle values (groups 1 and 3). Although these results are only for a limited number of allowed conformational states, it is apparent that there may be a larger number of similar conformations where the classical definitions of phi and psi are used in a full phi/psi conformational search. For example, if the full range of phi/psi conformational states is used in a simulation with 1-degree torsion angle increments, each residue can have a total of 129,600 (360×360) conformations. However, taking peptide plane rotation into account, there are 360 conformational states (using 1-degree increments) that are similar for every residue. This means that there are actually only 360 unique conformations per residue ($360 \times 360/360$) compared to 129,600 for the full range of allowed conformations.

Simplified Model—A Single Torsion Angle Conformational Variable

Based on the observation that anticorrelated torsion angle changes in peptide plane rotation describe similar conformations for multiple values of phi/psi, a new simplified representation of the protein backbone in computer simulations of protein folding is defined. Because there are certain values of phi and psi that describe groups of conformations related by peptide plane rotation, it is proposed that the phi and psi values related to only peptide plane rotations can be separated from phi and psi values that produce large global conformational changes in the protein structure. In other words, the observed distribution of conformational states, represented as phi/psi torsion angles, can be decomposed into two components. One component is the conformational torsion angle related to large global changes. The second component is the peptide plane rotation angle, which describe different values of phi and psi within similar global conformations.

The torsion angle component that determines global conformational changes, can be described by anticorrelated changes in the values of $\text{psi}(i) = -\text{phi}(i+1)$ on one of several diagonal lines parallel to those shown in Figure 1. Using the right-hand helix as a reference point, all dipeptide conformations with the value of $\text{psi}(i, -40) + \text{phi}(i+1, -60) = -100$, from the alpha helix values (line A in Fig. 1) will have similar conformations. This summed value of -100 is called the frame-shifted equivalent value. This means that the following dipeptide conformations will be similar, $-40/-60$, $0/-100$, $40/-140$, $80/-180$ (all values on line A in Fig. 1) as well as any other conformations with $\text{psi}(i)$ and $\text{phi}(i+1)$ values that fall on line A (Table II). In another example, any dipeptide in an extended conformation with $\text{psi}(i, 140) + \text{phi}(i+1, -140) = 0$ (line C in Fig. 1) will be similar, and any dipeptide in a left-hand helix conformation

with psi(i, 40) + phi(i + 1, 60) = 100 (line B in Fig. 1) will have similar conformations. For any torsion value the corresponding frame-shifted values to plot frame-shifted contour plots can be derived by using a frame-shifted equivalent value equal to the sum of psi(i) and phi(i + 1).

For conformations related by a peptide plane rotation, one value of either phi or psi can be selected as a reference conformation to remove or freeze peptide plane rotation in a protein folding simulation. The remaining value of psi or phi, can then be used to describe global conformational changes. In this article, the right-hand helix conformation ($-60/-40$) is used as a reference conformation where phi is fixed at -60. All values of phi(i + 1) are set equal to -60, and the corresponding psi(i) values are modified using the rule psi(i) = $-$phi(i + 1) as described above. As an example, the frame-shifted or projected contours lines for similar conformations of all Rooman dipeptide torsion angles listed in Table II are shown in Figure 4, and were derived using the frame-shifted equivalent values described above. A comparison of these Rooman dipeptide conformational angles and the equivalent frame-shifted angles derived from the Rooman angles, where phi is set to -60 degrees, is listed in Table III. The frame-shifted angles correspond to the psi values where the dotted (phi = -60) line shown in Figure 4 crosses the contour lines for each Rooman angle (squares in Fig. 4). A frame-shifted torsion value can be visualized from the frame-shifted contour plot in Figure 4 by selecting a torsion value, for example, the torsion value in conformation 1 in Table III ($140/-117$), and following the corresponding diagonal containing this point, to the dotted (phi = -60) line to give the frame-shifted value of $83/-60$ (see Table III).

The conformation torsion angle values (numbers 1–18) for groups 1 and 3 are listed in the top half of Table III, while the values (numbers 19–36) for groups 2 and 4 are listed in the bottom half of Tables III. Structures generated with these frame-shifted torsion angle values were compared to the original Rooman conformations (see Fig. 3) by superimposing the peptide plane atoms. The low RMSD values listed in Table III show that the Rooman and frame-shifted conformations 1–12 in group 1 are similar. This is also seen for the Rooman and frame-shifted conformations 19–30 in group 2. Although the higher RMSD values for conformations 13–18 in group 3 and 31–36 in group 4 are a result of the nearly 180 degree peptide plane flip from Rooman to frame-shifted

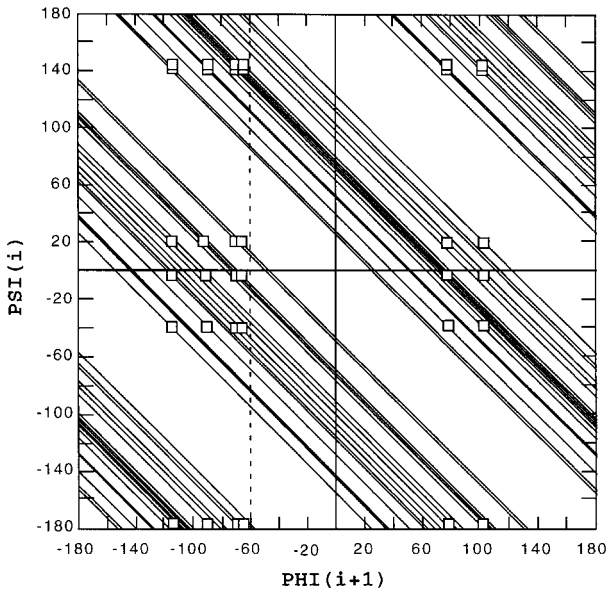

FIGURE 4. Dihedral angle frame-shifted plot of psi(i) (ordinate) and phi(i + 1) (abscissa) for all of the Rooman conformational torsion values (open squares) listed in Table II. Two major conformational groups can be seen. One conformational group is similar to the alpha-helix contour lines labeled A shown in Figure 1. The second conformational group is similar to conformations between the contour lines labeled C and B in Figure 1. The contour lines at the top right in Figure 4 are a continuation of the alpha-helix contour lines similar to the line labeled A in Figure 1. The contour lines at the bottom left in Figure 4 are a continuation of the extended and left-hand alpha-helix contour lines similar to the area between the lines labeled C and B in Figure 1, respectively.

conformations, the global conformations are similar. These comparisons show that all of the Rooman conformations in groups 1 to 4 are similar to their corresponding projected-angle conformations.

All of the Rooman conformations can then be described by projected or frame-shifted angles using only the value of psi for each residue. The diagonal lines in Figure 4 show the extensive phi/psi conformational space covered by these projected or frame-shifted angles, because all of the Rooman conformational angle values (squares in Fig. 4) as well as any conformation with phi and psi values that fall on one of the corresponding contour lines containing the Rooman value, are similar to the frame-shifted conformation value (psi) at phi = -60 on that line. Two major conformational groups are clearly seen in Figure 4. One group is represented by right-hand alpha-helix conformations, which are similar to the conformations described by psi(i)/ phi(i + 1) angles on the

TABLE III.

	Rooman		Frame Shifted		
Number	psi(i)	phi($i+1$)	psi(i)	phi($i+1$)	RMSD
1	140	−117	83	−60	0.5095
2	142	−117	85	−60	0.5095
3	−176	−117	127	−60	0.5073
4	140	−89	111	−60	0.2646
5	142	−89	113	−60	0.2637
6	−176	−89	155	−60	0.2605
7	140	−69	131	−60	0.0827
8	142	−69	133	−60	0.0827
9	−176	−69	175	−60	0.0805
10	140	−65	135	−60	0.0464
11	142	−65	138	−60	0.0424
12	−176	−65	179	−60	0.0453
13	−40	78	98	−60	1.0729
14	−1	78	137	−60	1.0921
15	20	78	158	−60	1.1042
16	−40	103	123	−60	1.1630
17	−1	103	162	−60	1.1812
18	20	103	−177	−60	1.1904
19	−40	−117	−97	−60	0.4882
20	−1	−117	−58	−60	0.4898
21	20	−117	−37	−60	0.4911
22	−40	−69	−69	−60	0.2519
23	−1	−69	−30	−60	0.2538
24	20	−69	−9	−60	0.2538
25	−40	−89	−49	−60	0.0783
26	−1	−89	−10	−60	0.0876
27	20	−89	11	−60	0.0791
28	−40	−65	−35	−60	0.0853
29	−1	−65	−6	−60	0.0445
30	20	−65	25	−60	0.0825
31	140	78	−82	−60	1.0614
32	142	78	−80	−60	1.0605
33	−176	78	−38	−60	1.0651
34	140	103	−57	−60	1.1591
35	142	103	−55	−60	1.1593
36	−176	103	−13	−60	1.1756

All 36 dipeptide torsion values using six conformations per residue as described by Rooman listed in column 2 with the corresponding frame-shifted torsion values in column 3. The all-atom RMSD for the Rooman conformations superimposed onto the frame-shifted conformation is listed in column 4.

contour line labeled A in Figure 1. The second group of conformations is represented by extended and left-hand alpha-helix conformations, which are similar to the conformations described by psi(i)/phi($i+1$) angles on the contour lines between C and B in Figure 1. Although this single projected angle representation for each residue is similar to the reduced number of variables used in conformational search methods for the virtual bond or pseudodihedral angle model,[12, 13, 15] this model retains a full atom description of residues in a protein sequence. As shown for the Rooman conformation database, only a limited number of torsion angles in the form of projected or frame-shifted psi values may be required in protein folding simulations.

Conclusion

The direction of the growing peptide main chain, defined as the direction of N(i)—CA(i) and CA($i+1$)—CO($i+1$) for dipeptides, is similar for many conformations that are related by anticorrelated torsion angle changes with peptide plane rotation. Peptide plane rotation shows that the large conformational search space of phi and psi values (Levinthal Paradox) can be projected to a substantially smaller frame shifted search space by using a single frame-shifted torsion angle value for each residue. The results presented in this article suggest that if torsion angles are used to compare protein conformations,[43] different torsion angles do not necessarily mean that different global conformations are involved. For example, motif database or torsion angle databases[21] derived from phi and psi torsion angles will contain a significant amount of redundant information because many conformations are related by peptide plane rotation.

The implications of the crucial role of peptide plane rotation and the use of frame-shifted torsion angle values will be investigated in several areas of protein folding,[44] in the calculation of conformational energies of native structures (thermodynamic hypothesis), in the range of conformational search space spanned, and in the physical measurements that depend on the orientation of the peptide plane, such as CD, NMR, and hydrogen bond exchange. The use of a frame-shifted or one torsion angle variable will also be examined to provide a one-dimensional display of protein conformation,[45] where currently the two-dimensional Ramachandran plot is used to visualize the three-dimensional structure of a protein. Protein folding simulations with one torsion angle variable provide the advantages of full atom simulation using an internal coordinate system with a reduced number of search variables. It remains to be seen whether this proposal of peptide plane rotation is only a convenient tool to describe a more efficient

conformational search method, or whether this is a real physical process to describe a subset of local motions in proteins.

References

1. Anfinsen, C. B. Science 1973, 181, 223.
2. Levinthal, C. In Mossbauer Spectroscopy in Biological Systems; Debrunner, P.; Tsibris, J. C. M.; Munck, E., Eds.; Proceedings of a meeting held at Allerton House, March 17 and 18, Monticello, Illinois, University of Illinois Press, 1969, p. 22.
3. Dill, K. S. Biochemistry 1985, 24, 1501.
4. Zwanzig, R.; Szabo, A.; Bagghi, B. Proc Natl Acad Sci USA 1992, 89, 20.
5. Ngo, J. T.; Marks, J.; Karplus, K. In Protein Folding Problems and Tertiary Structure Prediction; Mertz, K., Jr.; LeGrand, S. Eds.; Birkhauser, Boston, 1994, p. 433.
6. Scheraga, H. A. Review of Computive Chemistry; Lipkowitz, K. B.; Boyd, D. B., Eds.; VCH Publishers, Inc., New York, 1992, p. 73, vol. 3.
7. Gibson, K. D.; Scheraga, H. A. J Comp Chem 1994, 15, 1403.
8. Vasquez, M.; Nemethy, G.; Scheraga, H. A. Chem Rev 1994, 94, 2183.
9. Lee, B.; Kurochkina, N.; Kang, H. S. FASEB J 1996, 10, 119.
10. Meza, J. C.; Judson, R. S.; Faulkner, T. R.; Tresurywala, A. M. J Comp Chem 1996, 17, 1142.
11. Fischer, D.; Rice, D.; Bowie, J. U.; Eisenberg, D. FASEB J 1996, 10, 126.
12. Levitt, M. J Mol Biol 1976, 104, 59.
13. McCammon, J. A.; Northrup, S. H. Biopolymers 1980, 19, 2033.
14. Wilson, C.; Doniach, S. Proteins 1989, 6, 193.
15. DeWitte, R. S.; Shakhnovich, E. I. Protein Sci 1994, 3, 1570.
16. Turner, J.; Weiner, P.; Robson, B.; Venugopal, R.; Schubele, H., III; Singh, R. J Comp Chem 1995, 16, 1271.
17. Karplus, M.; Weaver, D. L. Protein Sci 1994, 31, 650.
18. Dill, K. A.; Bromberg, S.; Yue, K.; Fiebig, K. M.; Yee, D. P.; Thomas, P. D.; Chan, H. S. Protein Sci 1995, 4, 561.
19. Rice, L. M.; Brunger, A. T. Proteins Struct Funct Genet 1994, 19, 277.
20. Sippl, M. J. J Mol Biol 1990, 213, 859.
21. Rooman, M. J.; Kocher, J. P. A.; Wodak, S. J. J Mol Biol 1991, 221, 961.
22. Brasseur, R. J Mol Graphics 1995, 13, 312.
23. Avbelj, F.; Moult, J. Proteins 1995, 23, 129.
24. Sun, S.; Thomas, P. D.; Dill, K. A. Protein Eng 1995, 8, 769.
25. Srinivasan, R.; Rose, G. D. Proteins 1995, 22, 81.
26. Evans, J. S.; Mathiowetz, A. M.; Chan, S. I.; Goddard, W. A., III. Protein Sci 1995, 4, 1203.
27. Cheng, B.; Nayeem, A.; Scheraga, H. A. J Comp Chem 1996, 17, 1453.
28. Engh, R. A.; Huber, R. Acta Crysallogr 1997, 47, 392.
29. Laskowski, R. A.; Moss, D. S.; Thorton, J. M. J Mol Biol 1993, 231, 1049.
30. Ramachandran, G. N.; Sasisekharan, V. Adv Protein Chem 1968, 23, 283.
31. Richardson, J. S. Adv Protein Chem 1981, 34, 167.
32. Go, N.; Scheraga, H. A. Macromolecules 1970, 3, 178.
33. Elofsson, A.; LeGrand, S. M.; Eisenberg, D. Proteins 1995, 23, 73.
34. Peticolas, W. L.; Kurtz, B. Biopolymers 1980, 19, 1153.
35. Balasubramanian, R. Biochem J 1976, 157, 769.
36. Sudarsanam, S.; DuBose, R. F.; March, C. J.; Srinivasan, S. Protein Sci 1995, 4, 1412.
37. Geetha, V.; Munson, P. J. J Biomol Struct Dynam 1996, 13, 781.
38. Ball, J.; Andrew, P. R.; Alewood, P. F.; Hughes, R. A. FEBS 1990, 273, 15.
39. Palmer, K. S.; Scheraga, H. A. J Comp Chem 1991, 12, 505.
40. McCammon, J. A.; Gelin, B. R.; Karplus, M. Nature 1977, 267, 585.
41. Blackledge, M. J.; Bruschweiler, A.; Griesinger, C.; Schmidt, J. M.; Xu, P.; Ernst, A. N. Biochemistry 1993, 33, 10960.
42. Karplus, P. A. Protein Sci 1996, 5, 1406.
43. Korn, A. P.; Rose, D. R. Protein Eng 1994, 7, 961.
44. Honig, B.; Cohen, F. Folding Design 1996, 1, R17.
45. Parker, J. M. R. High Performance Computing Systems and Applications 98, 12th Annual International Symposium, poster, Edmonton, Alberta, Canada, May 20–22, 1998.